Novel closed-head, awake model of repetitive concussion with momentary loss of consciousness in mice

Eric Brengel, M.S.; Shreyas Balaji; Praveen Kulkarni, Ph.D.; & Craig Ferris, Ph.D.
Center for Translational Neuroimaging, Northeastern University, Boston, MA

Northeastern University
Center for Translational Neuro-imaging

PSTR336.01/W7

Introduction

Mild traumatic brain injury (mTBI), commonly known as concussion, is the most prevalent form of head trauma, with over 40 million injuries estimated per year worldwide[1]. Of particular concern are cases of repetitive concussion (rmTBI), a risk factor for neurodegenerative disease onset later in life[2]. In order to develop treatments and better understand the mechanisms underlying neurodegenerative risk, preclinical models must be developed with maximal translational value. In pursuit of this aim, our lab has adapted the existing momentum exchange model of repetitive concussion[3,4] for use in conscious mice.

Experimental Design

The following procedures were used to validate the adapted momentum exchange model in a multimodal fashion, utilizing behavioral assays, *in vivo* structural and functional neuroimaging, and *ex vivo* histology. Young adult (PD 90) C57BL/6 mice (*N*=24, 50% male) were housed in a reverse light-dark cycle with all procedures executed during the active (dark) phase under dim red light.

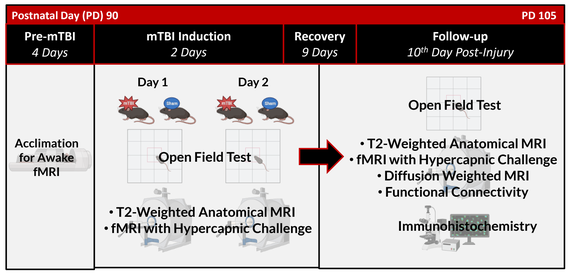

Momentum Exchange Model

The momentum exchange method ranks highly among mTBI models in translational value for its ability to generate tightly regulated, ecologically valid linear and rotational forces without skull fracture; however, it has only been used in rats, limiting accessibility of its use for longitudinal, transgenic, and exploratory studies[5]. In this adaptation, each mouse is lightly anesthetized with isoflurane and administered 1 mg/kg buprenorphine before being secured in the holding tube via bite bar and fitted with a 3 mm resin-polyurethane helmet. Upon arousal, the pneumatic impactor is propelled, creating rotational acceleration around the tube's hinge and linear acceleration along the platform's chassis.

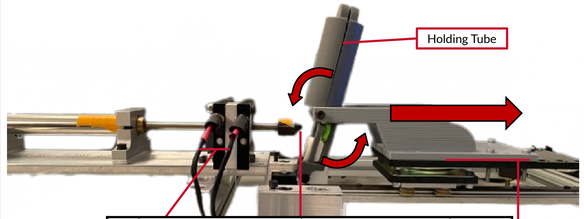

N	Mean Impact Velocity ± SD	Mean Energy Input ± SD	Mortality
22	3.677 ± 0.107 m/s	0.338 ± 0.020 J	0%

Loss of Consciousness

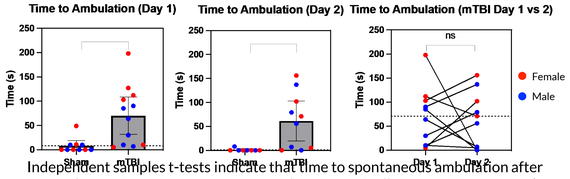

Independent samples t-tests indicate that time to spontaneous ambulation after removal from the apparatus is significantly increased following mTBI on Day 1 (p = 0.005) and Day 2 (p = 0.010), suggesting momentary loss of consciousness. Paired samples t-test indicates there is no significant change in time to ambulation after a second impact (p = 0.743).

No Changes in Locomotor Behavior

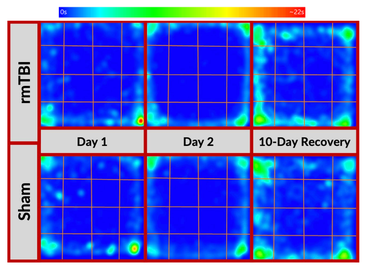

Half of all mice underwent a 5-minute Open Field Test on Day 1, half on Day 2, and all were repeated on the 10th day of recovery. Group average heat maps are shown. Cross-sectional independent samples t-tests indicate no significant effect of condition at any timepoint (p > 0.05).

No Changes in Gross Anatomy or Evidence of Skull Fracture

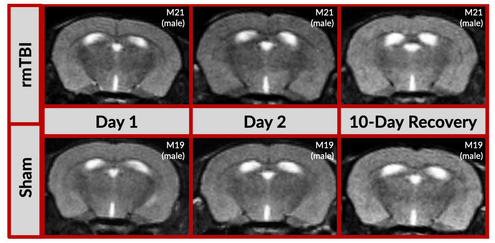

T2-weighted scans of representative mice following mTBI or sham procedures

Highlights

By adapting the momentum exchange model of rmTBI for use in mice, translational studies employing longitudinal, transgenic, and exploratory designs will become more accessible to preclinical researchers

Model Features
- Closed-head impact
- Allows for use in conscious mice during the active phase
- Linear and rotational acceleration
- Intertrial consistency
- No mortality

Model Outcomes
- Momentary loss of consciousness
- No changes in locomotor behavior
- No changes in gross anatomy or evidence of skull fracture
- Altered neurovascular coupling emerges after repetitive injury and partially recovers in 10 days
- Cytotoxic edema evident 10 days after repetitive injury

Neurovascular Coupling is Altered by Repetitive (but not Single) mTBI and Partially Recovers in 10 Days

fMRI with Hypercapnic Challenge

CO2 Challenge: Positive BOLD Volume of Activation Immediately Following One Hit				
Brain Area	Sham		1 Hit	P val
infralimbic ctx	5	>	0	0.004
stria medullaris	1	>	0	0.017
locus ceruleus	0	<	2	0.019

CO2 Challenge: Positive BOLD Volume of Activation Immediately Following Two Hits				
Brain Area	Sham		2 Hit	P val
globus pallidus	29	<	109	0.004
reticular thalamic n.	25	<	46	0.004
secondary somatosensory ctx	57	<	225	0.004
anterior thalamic n.	22	<	63	0.007
CA1	141	<	338	0.007
retrosplenial rostral ctx	111	<	177	0.007
ventral thalamic n.	119	<	226	0.007
dentate gyrus	170	<	272	0.007
primary somatosensory ctx	279	<	832	0.007
visual 1 ctx	280	<	545	0.007
extended amydala	11	<	33	0.009
vestibular n.	89	<	119	0.009
rostral piriform ctx	115	<	327	0.009
prelimbic ctx	44	<	60	0.009
paraventricular thalamic n.	5	<	19	0.011
central medial thalamic n.	15	<	21	0.011
auditory ctx	70	<	159	0.012
anterior pretectal thalamic n.	10	<	28	0.012
CA3	48	<	134	0.012
flocculus cerebellum	60	<	176	0.012
insular rostral ctx	49	<	230	0.012
subiculum	163	<	286	0.012
superior colliculus	222	<	353	0.012
cerebellar nuclear n.	34	<	65	0.015
medial geniculate	27	<	52	0.018
lateral rostral hypothalamic n.	51	<	124	0.018
primary motor ctx	78	<	206	0.018
orbital ctx	150	<	233	0.018
posterior thalamic n.	23	<	39	0.018
bed nucleus stria terminalis	31	<	66	0.018
caudate putamen	264	<	726	0.019
gigantocellilaris reticular n.	173	<	241	0.019
medial amygdaloid n.	27	<	82	0.019
dorsal medial hypothalamic n.	7	<	12	0.022
10th cerebellar lobule	22	<	35	0.028
central amygdaloid n.	21	<	71	0.028
cortical amygdaloid n.	53	<	163	0.028
pontine reticular nucleus oral	123	<	163	0.028
ventral pallidum	32	<	74	0.028
2nd cerebellar lobule	24	<	65	0.028
5th cerebellar lobule	89	<	128	0.028
entorhinal ctx	258	<	622	0.028
frontal association ctx	56	<	120	0.028
secondary motor ctx	83	<	218	0.028
reticular formation	186	<	287	0.028
reuniens thalamic n.	11	<	27	0.031
4th cerebellar lobule	26	<	37	0.034
ventral medial hypothalamic n.	11	<	24	0.034
lateral posterior thalamic n.	16	<	31	0.041
pontine n.	71	<	103	0.041
accumbens shell	45	<	59	0.042
lateral caudal hypothalamic n.	28	<	45	0.042
zona incerta	28	<	36	0.042
anterior olfactory n.	163	<	300	0.042
basal amygdaloid n.	31	<	124	0.042
temporal ctx	10	<	68	0.042

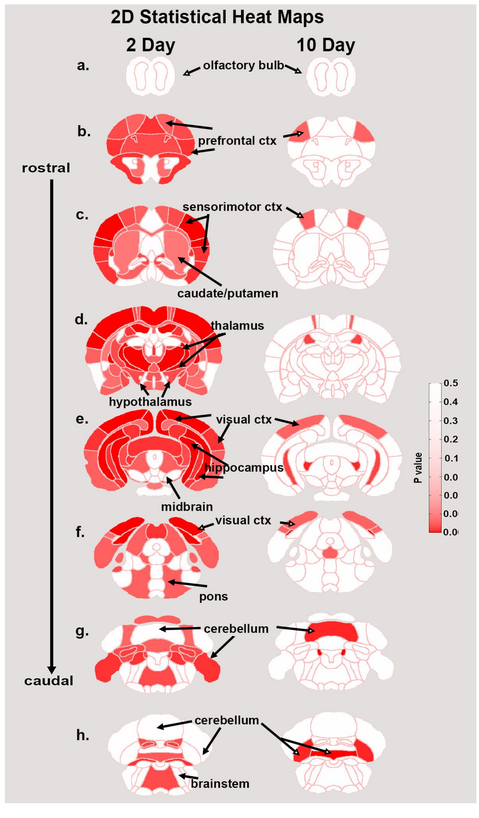

CO2 Challenge: Positive BOLD Volume of Activation Following 10 Days of Recovery from Two Hits				
Brain Area	Sham		2 Hit	P val
locus ceruleus	2	<	4	0.009
10th cerebellar lobule	25	<	33	0.009
lateral reticular n.	22	>	0	0.011
dorsal hippocampal commiss.	16	>	7	0.011
anterior pretectal thalamic n.	12	<	24	0.013
3rd cerebellar lobule	43	>	9	0.014
olivary complex	9	<	27	0.014
5th cerebellar lobule	78	<	163	0.014
paramedian lobule	84	<	110	0.014
lateral preoptic n.	9	>	7	0.024
parafascicular thalamic n.	3	>	2	0.027
CA3	65	<	101	0.027
dorsal raphe	26	>	12	0.045
paraventricular hypothalamic n.	5	<	2	0.046
lateral posterior thalamic n.	15	<	26	0.049
primary motor ctx	177	>	127	0.050
temporal ctx	60	>	34	0.050
visual 1 ctx	429	>	360	0.050
6th cerebellar lobule	211	>	139	0.063
4th cerebellar lobule	33	<	36	0.084
7th cerebellar lobule	76	>	60	0.085
9th cerebellar lobule	58	>	37	0.085

Non-parametric Kruskal-Wallis tests of 140 brain regions indicate significantly altered BOLD signal in response to 5% CO_2 challenge in the regions listed (p < 0.05). The median number of voxels activated per region is shown in accompanying tables.

Thirty minutes after a single mTBI, alterations to neurovascular coupling are minimal.

Thirty minutes after a second mTBI within 24 hours, robust alterations to neurovascular coupling are observed diffusely.

Ten days after injury, alterations to neurovascular coupling are primarily limited to the cortex and cerebellum, indicating partial recovery.

Cytotoxic Edema 10 Days After Repetitive mTBI

Diffusion Weighted Imaging

Table: Significant Differences in Fractional Anisotropy at 10 Day Post 2 Hits

Fractional Anisotropy 10 Days Post 2 Head Impacts							
	Sham		2 Hits				
Brain Area	AVE	SD		Ave	SD	P val	Ω Sq
6th cerebellar lobule	0.43	0.07	>	0.32	0.01	0.014	0.705
pontine n.	0.40	0.02	>	0.36	0.02	0.014	0.705
simple lobule cerebellum	0.36	0.03	>	0.32	0.01	0.014	0.697
9th cerebellar lobule	0.43	0.06	>	0.31	0.04	0.019	0.616
vestibular n.	0.41	0.03	>	0.33	0.04	0.019	0.610
glomerular layer	0.35	0.03	>	0.30	0.02	0.024	0.553
pontine reticular n. caudal	0.34	0.02	>	0.28	0.04	0.024	0.553
4th cerebellar lobule	0.42	0.04	>	0.35	0.03	0.027	0.528
7th cerebellar lobule	0.48	0.07	>	0.36	0.02	0.027	0.522
granular cell layer	0.31	0.07	>	0.26	0.01	0.030	0.503
10th cerebellar lobule	0.35	0.04	>	0.27	0.05	0.036	0.458
cuneate n.	0.47	0.02	>	0.37	0.06	0.036	0.458
prepositus n.	0.37	0.06	>	0.27	0.05	0.037	0.452
fimbria hippocampus	0.56	0.03	>	0.50	0.06	0.048	0.387
ventral tegmental n.	0.36	0.03	>	0.29	0.06	0.048	0.387
posterior hypothalamic n.	0.33	0.04	>	0.27	0.05	0.049	0.382

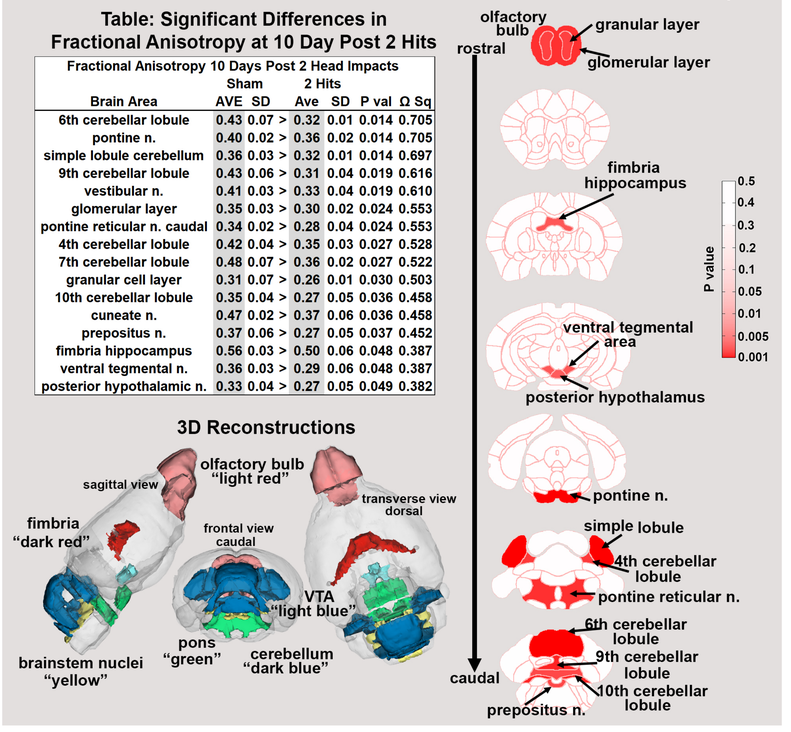

Non-parametric Kruskal-Wallis tests of 140 brain regions indicate significantly reduced fractional anisotropy 10 days after rmTBI in the regions listed (p < 0.05). Notable clusters of reduced fractional anisotropy include the cerebellum and olfactory bulbs. This suggests alterations to the microstructure of these regions that could be indicative of cytotoxic edema.

Future Directions

- **Functional Connectivity:** Analysis of Day 10 awake functional connectivity scans is underway to identify and characterize lasting changes to neurocircuitry.
- **Neuroinflammation:** Immunohistochemical analysis of brain tissue collected after Day 10 scanning is underway to identify lasting astrocytosis and microgliosis. Sample images from a female rmTBI brain are shown. (Left: GFAP⁺ astrocytes in the hippocampus. Right: IBA1⁺ microglia in the hippocampus)
- **Sex Differences:** Mixed-sex cohorts were used for this analysis[6]. Future studies with larger sample sizes will maintain this study design to allow for identification of sexual dimorphisms.
- **Longitudinal Studies:** This model will be used in future studies examining the interaction of rmTBI with lifestyle factors such as diet, exercise, and drug addiction as compounding neurodegenerative risk factors.

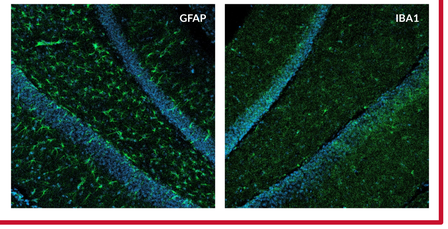

References & Acknowledgements

[1] Cassidy et al. (2004) *J Rehabil Med Suppl*
[2] Morissette et al. (2020) *Fam Med Com Health*
[3] Viano et al. (2009) *Neurosurgery*
[4] Kikinis et al. (2017) *Brain Inj*
[5] Angoa-Perez et al. (2014) *J Neurochem*
[6] Shansky (2019) *Science*

Scan to view our poster digitally:

Stay connected: brengel.e@northeastern.edu

EKAM
- 3D-printed holster components designed by Elizabeth Ling, M.S. and Atul Phadke.
- 3D-printing services provided by the Northeastern University 3D Printing Studio.
- Consultation and instrument support for confocal microscopy provided by the Institute for Chemical Imaging of Living Systems (RRID:SCR_022681).
- Special thanks to Ashley Ghaw and Deepti Athreya for their contributions to data collection and analysis.
- Financial support provided by Ekam Imaging.